RPE | Radiation Physics & Engineering
An International Peer-Reviewed Journal
Published by K.N. Toosi University of Technology
http://rpe.kntu.ac.ir
Research Article

Radiation Physics and Engineering 2020; 1(4):9–16
https://doi.org/10.22034/rpe.2020.104839

Differentiation method for Compton edge characterization in organic scintillation detectors

Mohammad Javad Safari

Department of Energy Engineering and Physics, Amir Kabir University of Technology, PO Box 15875-4413, Tehran, Iran

HIGHLIGHTS

- A simple and straightforward method for accurate characterization of Compton edge.
- Energy resolution of organic scintillation detectors.
- Estimating contribution of atomic bounded electrons via the Doppler effect in energy resolution of detectors

ABSTRACT

It is well-known that response function of organic scintillation detectors does not appear with photopeaks. Instead, their dominant feature is a continuum, usually called the Compton edge that innately exposes the resolution characteristics of detection system. While, accurate characterization of Compton edge is crucial for calibration purposes, it is also in charge of elaborating the energy resolution of detector. This paper presents a simple method for accurate characterization of the Compton edge in organic scintillation detectors. The method is based on the fact that differentiating the response function leads to accurate estimation of the constituting functions. The differentiation method, in addition to the location of the Compton edge, gives insights into the parameters of the folded Gaussian function which could lead to depict the energy resolution. Moreover, it is observed that the uncorrelated noise in the measurement of the response function does not impose significant uncertainties in the evaluations, so it could preserve its functionality even in lower-quality measurements. By simulation of the bounded electrons and considering the Doppler effects, we are able to demonstrate -the first ever- estimation for intrinsic Doppler resolution of an organic plastic scintillator. Even though, this possibility is an immediate result of benefiting the presented method for analysis of the Compton continua.

KEYWORDS

Compton edge
Response function
Detector calibration
Doppler resolution
Monte Carlo simulation

HISTORY

Received: 15 August 2019
Revised: 29 November 2019
Accepted: 3 December 2019
Published: October 2020

1 Introduction

Organic scintillators are usually calibrated by means of gamma-lines of radionuclide sources. Due to the low-Z content of the organic scintillators, their response is almost free of any photopeak, constituting a relatively wide Compton edge in the observed spectrum. One major obstacle to this goal, is to accurately determine location of the Compton edge. Several authors have proposed different methods, none of them met the requirements of a powerful procedure; as being accurate, fast and robust and simple. Usually, authors assume a specific location for the Compton edge, in comparison to the value of the count-rate at the local maximum, usually described by how much percent it deviates from the local maximum value. For example, Beghian et al. (Beghian et al., 1965) suggested 66%, Honecker and Grässler (Honecker and Grässler, 1967) suggested 70%, Bertin et al. (Bertin et al., 1969) suggested 85% to 87%, Knox and Miller (Knox and Miller, 1972) suggested 89%, and Swiderski et al. (Swiderski et al., 2010) proposed 78% to 82%. Nonetheless, this controversial suggestions has a root in the differences between the effective resolution of their detection systems (Safari et al., 2016). There are some alternative methods for partially overcoming such difficulties. For example, Chikkur and Umakantha (Chikkur and Umakantha, 1973), based on ad hoc arguments, have proposed to fit a Gaussian curve to the latter part of the spectrum, putting forward a way for relating the fitted parameters to the Compton edge.

To overcome the abovementioned difficulties, Dietze and Klein (Dietze, 1979; Dietze and Klein, 1982) have introduced a calibration procedure that is based on simulation of ideal response by means of a Monte Carlo code;

*Corresponding author: mjsafari@aut.ac.ir

convolving the simulated response into an assumed Gaussian function, with the hope that the convolved curve would find appropriate accommodation to the experimental data. Usually, finding the best conformity needs great deal of work, demanding several prediction/correction steps for evaluation of the appropriate Gaussian parameters or even considering the optical features of the detector (Kohan et al., 2012). Although, this method is not only able to determine the Compton edge, but also could define the energy resolution, it suffers from drawbacks, because it mostly relies on the users skills that demands several tedious iterations (Safari et al., 2016).

Here, based on simple mathematical arguments, a straightforward and accurate method will be presented to determine the Compton edge, as well as the detector resolution at that energy. The method, mostly benefited from the fact that an edge in the response could be modeled by a Heaviside step function (HSF), allowing one to find a simple explanation for the derivative of the response. This procedure, which is exploited in Sec. 2. Section 3, demonstrates the applicability of the method by examining some experimental measurements. Section 4 addresses a discussion about the simulation aspects of the Compton scattering, principally directed towards studying the Doppler resolution effects in the Compton scattering process. With the aid of the precision of the differentiation method, we are able to determine contribution of the Doppler effect quantitatively into the detector resolution. In this section, we have also addressed a comparison against the measured intrinsic resolution of organic scintillators (Swiderski et al., 2012; Roemer et al., 2010). Finally, some concluding remarks will be provided in Sec. 5.

2 Methods

Heaviside step function (HSF) described as follows

$$H(E)=\begin{cases}1 & E\le E_c\\ 0 & E>E_c\end{cases} \tag{1}$$

has the property that its derivative could be described by the Dirac delta function

$$\frac{\mathrm{d}}{\mathrm{d}E}H(E)=\delta(E-E_c) \tag{2}$$

Interestingly, it could be shown that the derivative of a Gaussian-folded HSF, is also a Gaussian function with similar parameters. Attributing the HSF as a representation of the recoiled proton spectrum, Kornilov et al. (Kornilov et al., 2009) have proposed a straightforward method for determination of the maximum recoiled proton energy in an organic scintillator. While the real-world spectrum is far from being a simple HSF, the method is proved to be accurate, because it is based on just a simple operation of differentiation. However, we have noticed that this aspect of the HSF could be generalized to every other disjoint function. This point will be elaborated below.

The measured spectra are subject to several sources of uncertainties (*i.e.* errors), which could be depicted by a Gaussian normal distribution. Most of these errors are uncorrelated, which make it meaningful to describe the whole set of broadening effects by means of a single Gaussian function with an overall estimation for its variance (σ). A Gaussian normal distribution could be written as

$$G(E)=\frac{1}{\sqrt{2\pi}\sigma}\exp(-\frac{E^2}{2\sigma^2}) \tag{3}$$

From a mathematical point of view, the *real* response function $R(E)$ emerges from convolution of the *ideal* response function $r(E)$ into the Gaussian distribution,

$$R(E)=r(E)\otimes G(E)=\int_{-\infty}^{\infty}r(x)G(E-x)\mathrm{d}x$$

The general theme of this work is based on the fact that frankly speaking the derivative of every disjoining function (like the HSF) behaves somehow like a Dirac delta or Gaussian functions. One simple and still useful model for an *ideal* Compton edge could be described by the following disjoint second-order function

$$r(E)=\begin{cases}aE^2+bE+c & E\le E_c\\ 0 & E>E_c\end{cases} \tag{4}$$

as visualized in Fig. 1. Its maximum value occurs at E_c, to have

$$r(E)=aE_c^2+bE_c+c \tag{5}$$

meaning that in an ideal system (*i.e.* not subject to the finite energy resolution effects), the Compton edge is exactly located at the local maximum of the response function. Inclusion of the resolution, demands the convolution of $r(E)$ into a corresponding Gaussian function (Eq. (3)), which results in

$$R(E)=\alpha_1.\mathrm{erfc}\Big[\frac{E-E_c}{\sqrt{2}\sigma}\Big]+\beta_1.\exp\Big[-\frac{(E-E_c)^2}{2\sigma^2}\Big] \tag{6}$$

where

$$\mathrm{erfc}(E)=1-\frac{2}{\sqrt{\pi}}\int_0^E \mathrm{e}^{-x^2}\,\mathrm{d}x$$

is the complementary error function, and the following conventions have been assumed as:

$$\begin{aligned}\alpha_1(E)&\equiv\frac{1}{2}\big[a(E^2+\sigma^2)+bE+c\big]\\ \beta_1(E)&\equiv\frac{-\sigma}{\sqrt{2\pi}}a(E+E_c)+b.\end{aligned} \tag{7}$$

This convolved response (standing for the real response function) is of smoother behavior, also displayed in Fig. 1. It is simple to verify that the value of $R(E)$ at the Compton edge could be obtained from the following relation:

$$\begin{aligned}R(E_c)&=\alpha_1(E_c)+\beta_1(E_c)\\ &=\frac{1}{2}r_{max}-\frac{1}{\sqrt{2\pi}}2aE_c+b\sigma+\frac{a}{2}\sigma^2\end{aligned} \tag{8}$$

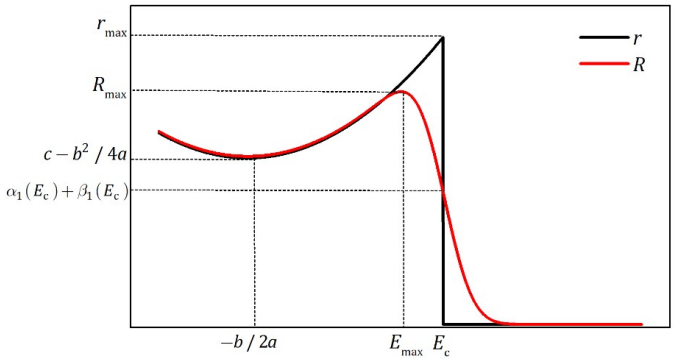

Figure 1: Ideal linear response function: $r(E)$, and the convolved response function: $R(E)$.

Equation (8) strictly shows that the half-value of (or some other percent of) $r_{\max}$ could not be considered as a universal measure of the Compton edge (E_c). It also indicates that a wider Gaussian resolution (*i.e.* increasing σ) shifts the local maximum to the left-hand-side of its original (correct) position, making a sense about the various heuristically reported values for the Compton edge location, described earlier in Sec. 1.

Differentiating $R(E)$ we find

$$R'(E) = X_1(E) + X_2(E) \tag{9}$$

where, we have accepted the following notation

$$\begin{aligned} X_1(E) &\equiv \alpha_2.\mathrm{erfc}\Big[\frac{E-E_c}{\sqrt{2}\sigma}\Big] \\ X_2(E) &\equiv \beta_2.\exp\Big[-\frac{(E-E_c)^2}{\sqrt{2}\sigma^2}\Big] \end{aligned} \tag{10}$$

and

$$\begin{aligned} \alpha_2 &\equiv \frac{1}{2}(2aE+b) \\ \beta_2 &= -\frac{1}{\sqrt{2\pi}\sigma}\Big[a(E_c^2+2\sigma^2)+bE_c+c\Big] \end{aligned} \tag{11}$$

The shape of these latter functions are illustrated in Fig. 2, and they pose interesting relations. Especially there is a constant slope at the rightmost, governed by X_1 as

$$\theta = a.\mathrm{erfc}\Big[-\frac{E_c}{\sqrt{2}\sigma}\Big] \tag{12}$$

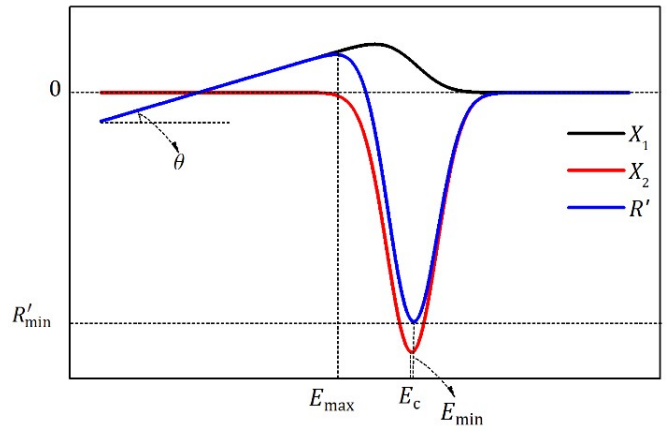

Figure 2: Differentiation of the response function ($R(E)$) and its constituting components (X_1 and X_2).

Although the shape of R' is mostly governed by X_2 (which certainly is a Gaussian distribution), one can conclude from Fig. 2 that the correct location of local minimum slightly differs from that of the X_2. The correct value of this minimum could be obtained by

$$E_{\min} \simeq E_c + \frac{b\sigma^2 - \sqrt{2\pi}a\sigma^3}{a(E_c^2-\sigma^2)+bE_c+c} \tag{13}$$

This necessitates a positive correction term (usually below 1%), as it also could be seen in Fig. 2. Moreover, this equation indicates that increasing the Gaussian variance (*i.e.* deteriorating the resolution), as well as decreasing the incident energy magnifies this correction term. Although, it is handy to approximate the Compton edge, solely by the local minimum of the X_2:

$$E_c \simeq E_{\min} \tag{14}$$

This approximation is acceptable for most interesting cases, because usually we have $\sigma \sim$1 keV, while $E_c \sim$10-100 keV, diminishing the correction term in these instances. Noting this, one is also able to calculate the approximate $R'_{\min} \approx R'(E_c)$ as

$$R'_{\min} = aE_c + \frac{b}{2} - \frac{1}{\sqrt{2\pi}\sigma}\big[a(E_c^2+\sigma^2)+bE_c+c\big].$$

This equation along with Eq. (12) could help to resolve the various features of the Compton edge completely.

3 Experiments

For experimental verification of the differentiation method, we have measured the response function of a ⌀2"×2" BC400 plastic scintillator (Scintillators, 2016) irradiated by three gamma-ray isotopic sources: Cs-137, Na-22 and Co-60 (See Table 1). Due to the lack of enough resolution to discriminate between distinct Co-60 gamma-lines, we assumed an average energy of 1252.8 keV for this source.

Usually, it is expected to observe statistical fluctuations in the response functions. Although, such fluctuations might be invisible, they could result in serious/larger fluctuations in the corresponding derivative. Figure 3 is the measured spectrum of Cs-137 (standing for 72 hours of irradiation by $\sim \mu$Ci source) along with its corresponding differentiation, revealing that whilst the response is apparently smooth, its derivative exhibits sizeable perturbations. Even though, it is notable that most of these fluctuations are of non-correlated nature and could be effectively eliminated by *low-pass filtering*, with appropriate windowing (here Blackman window) to keep the original progression of the data (Shenoi, 2005). The cut-off angular frequency (ω_c) of the low-pass filter could vary over the domain $[0, \pi]$, implying variation of the output, ranging from the no-pass (for zero) to all-pass (for π) filters. With the aid of a robust nonlinear fitting procedure, there would be no troubles in fitting, even with noisy data.

Table 1: Gamma-ray sources for experiments.

Nuclide	Cs-137	Na-22	Co-60
Energy (keV)	661.7	511.0 1274.5	1173.2 1332.5 Average: 1252.8
Exact Compton edge (keV)	447.0	339.0 1061.0	963.5 1332.5 Average: 1040.2
Estimated Compton edge (keV)	477.2±0.06	339.5±0.07 1061.0±0.05	- - Average: 1042.2±0.06
Correct location (%)	57.4	56.3 68.0	- - 65.1
Resolution (%)	14.06±0.01	15.96±0.01 11.97±0.02	- - 11.87±0.03

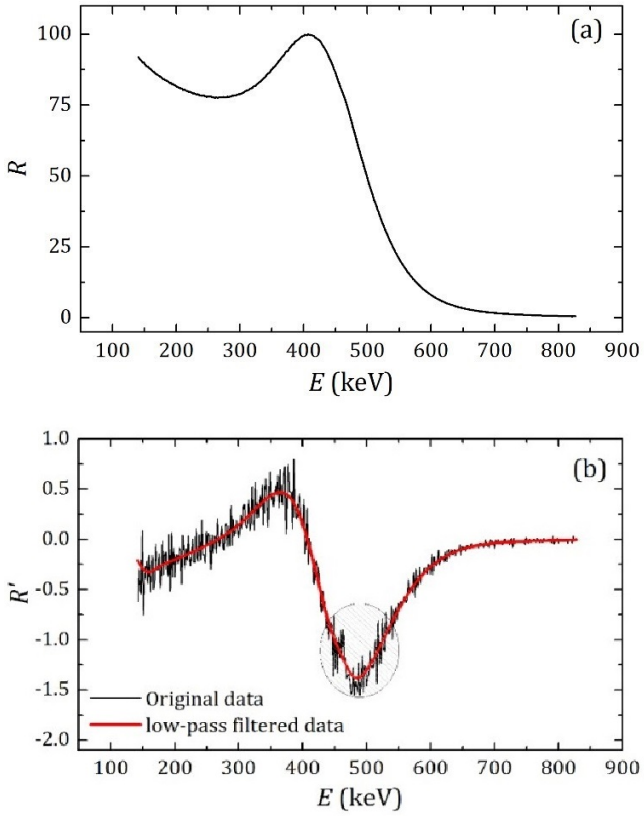

Figure 3: a) Measured response function for Cs-137 gamma-ray source. b) Derivative of the measured response function (thin black line), and low-pass filtered response function (thick red line).

Figure 4 demonstrates this point, because it shows that low-pass filter smoothing has no considerable effect on the outcome of the procedure (mostly about ±1%). This is somehow contrary to Kornilov et al. (Kornilov et al., 2009) and Stevanato et al. (Stevanato et al., 2011), whom found problems with raw (*i.e.* non-filtered) data. For the fitting purposes, one could focus on the central region around the appeared peak, which is useful to discard asymmetry effects of the data shown by shaded region in Fig. 3-b in the case of Cs-137. The accuracy of the method could be concluded from the results of Table 1. Furthermore, it explicitly shows that assuming a specific percentage of the local Compton maximum is not a correct representative of the Compton edge location. For example, the correct location is taking 80% of the maximum (as it is usually the case) that leads the deviation about 27 keV from the correct location in for Cs-137 peak.

After adjusting the calibration coefficient by means of the Na-22 peaks, we were able to predict the location of the Cs-137 and Co-60 gamma-lines, depicted in Fig. 5, appearing that the uncertainty of experimental data are practically invisible. Moreover, it could be seen that the approximate location of the effective gamma-rays of Co-60 are also acceptable within experimental errors. For comparison purposes, we made a comparison against some other experimental data reported by Jolivette and Rouze in Ref. (Jolivette and Rouze, 1994). These data were measured by an HPGe detector, so they are of higher quality (usually having about 1 keV reported uncertainties). The consistency and accuracy of results could be seen in Fig. 5 with a comparison against MCNPX simulations that are considered to come up with the exact value of edge location.

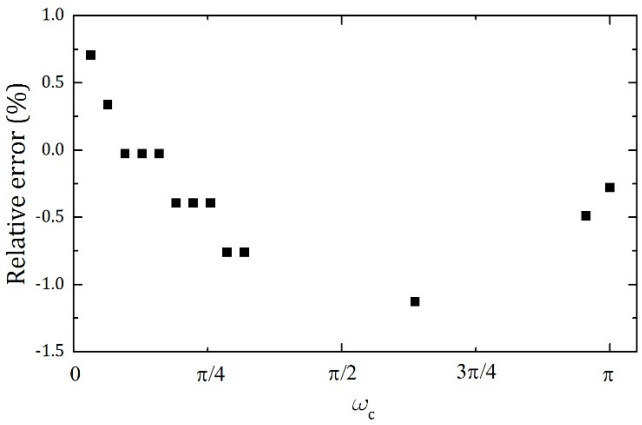

Figure 4: Relative error ($\frac{E_x - E_c}{E_c} \times 100$) in determination of the estimated Compton edge (E_x), after low-pass filtering with different cut-off frequencies (ω_c).

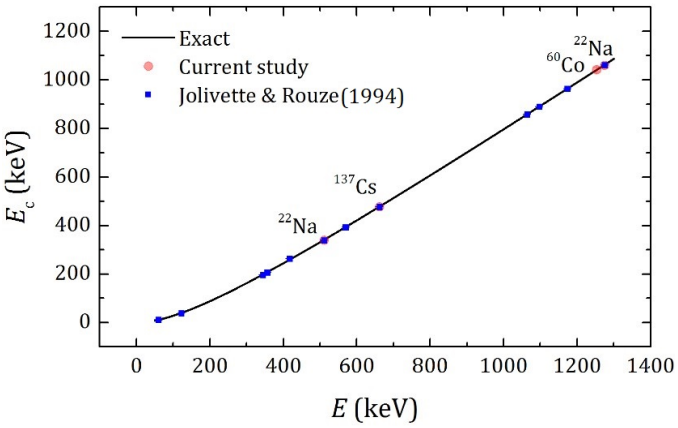

Figure 5: Compton edge location, as specified by the differentiation method (Current study), in comparison to the MCNPX (Exact) estimations and the measurements by Jolivette and Rouze (Jolivette and Rouze, 1994).

4 Doppler resolution

Bounded atomic electrons are not at rest, making certain deviations from the free-electron assumption in derivation of the conventional Klein-Nishina cross sections (Cooper, 1997). This boundedness results in Gaussian broadening of the energy-angle distribution of the outgoing entities usually referred to as the Doppler broadening (Williams, 1977). It is well-known and well-documented that this Compton scattering usually implies a finite Doppler resolution in the energy distribution of the detector's response function (Knoll, 2010). Notwithstanding, this Doppler resolution completely differs from other contributing effects in the total energy resolution of a scintillation detector (such as the light generation and transport effects, electronic noise/fluctuations effects, *etc.*), revealing a situation somehow similar to the intrinsic resolution which is anticipated in the case of inorganic scintillators. This property could be asserted by intuitive arguments. However, up to our knowledge, there is no quantitative analysis, which is deemed to be due to the lack of a precise enough method for accurate localization of the Compton edge. Here in this section, we are aiming to resolve this issue by employing the differentiation method and benefiting its accuracy in characterization of the Compton edge properties.

Most of the modern radiation transport simulation codes have certain capabilities to handle low-energy photon interactions perceiving the momentum distribution of bounded electrons. For example, there were immense efforts to develop such a capability in GEANT4 (Kippen, 2004; Brown et al., 2014), FLUKA (Böhlen et al., 2012; Kling et al., 2014), EGS4 (Namito et al., 1994, 1998, 1993), PENELOPE (Brusa et al., 1996; Sempau et al., 1997; Salvat and Fernández-Varea, 2009; Salvat et al., 2006), and especially in MCNPX (Briesmeister, 2000; Pelowitz et al., 2005).

MCNPX/5 is a multi-purpose Monte Carlo simulation code (Pelowitz et al., 2005) with the capability to handle bounded electrons (Sood, 2004; Sood and White, 2004; Sood, 2009). Here in this study, we were made use of the MCNPX code to simulate the response function, taking note of the shortcomings of its previously released photons cross section library (White, 2002, 2003), hence considering its more recent data set (White, 2012).

Considering an ideal ⌀2"×2" cylindrical BC400 plastic scintillator, we have performed the simulations reported below. According to the BC400 datasheet (Scintillators, 2016) the material composition were fixed to H/C:1.103, mass density: 1.032.

Before consulting to the detector simulation issue, we checked the simulation of bounded electrons for 500 keV (Fig. 6) and 30 keV (Fig. 7) gamma-rays initially, by considering the Compton interaction in a tiny sample ($\sim 10^{-5}$ cm) of the plastic scintillator. Taking such a tiny sample is to be avoided re-collision of incident and outgoing photons. As a matter of study, we have calculated intensity of the outgoing photons as a double-differential function of energy and angle. These figures explicitly show the broadening at different angles and energies, and clearly depicts that it is not uniform in all outgoing energy/angles (see Fig. 7-b).

Employing the *differentiation method* for analysis of the simulated spectra, we were able to determine the FWHM and subsequently obtain the corresponding energy resolution (Fig. 8). One should note that these are exclusively resulted from the (Doppler broadening of the) bounded electron effects. The relation between resolution (ε), the FWHM and the variance of the Gaussian peak (σ) is the following well-known equation (Knoll, 2010)

$$\varepsilon(\%) = \frac{\mathrm{FWHM}}{E_0} = 200\sqrt{2\ln 2}\,\frac{\sigma}{E_0} \tag{15}$$

Fitting the Doppler resolution using a power model function of the form

$$\varepsilon = \alpha E^{\beta} \tag{16}$$

We find $\alpha = 477.5 \pm 0.03$ and $\beta = -1.02 \pm 0.02$, persuading the $1/E$ relation for the Doppler resolution. It is noteworthy that the error (Relative error in every fitted curve has been calculated with the following equation: $100 \times (\varepsilon - \varepsilon_{\mathrm{Fit}})/\varepsilon$) in the fitted curve is mostly below 25%, while it is more accurate at lower energies (below ~300 keV), depicted in the dashed region of Fig. 8-b.

The estimated Doppler resolution varies from 1.5% to 45% for incident photons of energies below about 300 keV down to 10 keV. This has a strict implication, urging to incorporate the Doppler broadening -or detailed physics model in terms of the MCNPX nomenclature- into the simulations. One should not forget that the detailed physics model of the MCNPX code is disabled by default. Swiderski et al. have studied the intrinsic resolution of organic scintillators (Swiderski et al., 2012), taking *all possible effects* into account. Their measurements for BC408 resulted in a set of data which are firmly consistent with the fitting of power model Eq. (16), with $\alpha = 139.11 \pm 0.02$ and $\beta = -0.496 \pm 0.1$. This result is very close to the $1/\sqrt{E}$ relation, as it could be anticipated by noting the well-known role of the statistical uncertainty in the en-

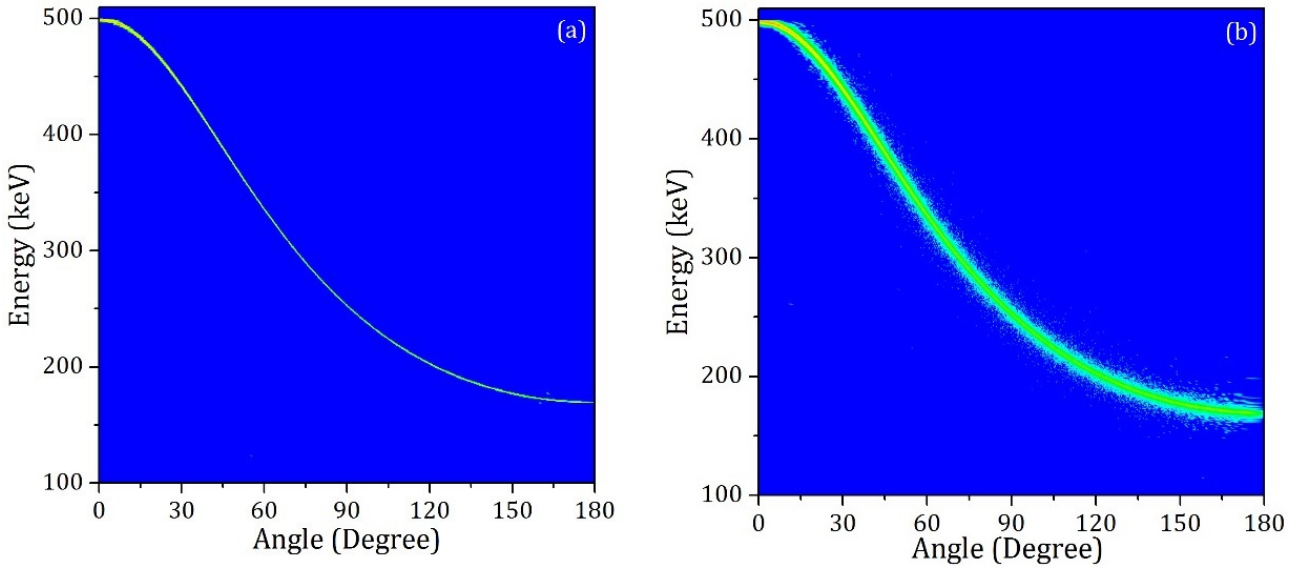

Figure 6: Double-differential distribution of the outgoing flux of gamma-rays as a function energy and angle, for incident photon $E = 500$ keV, a) without and, b) with the bounded electron model.

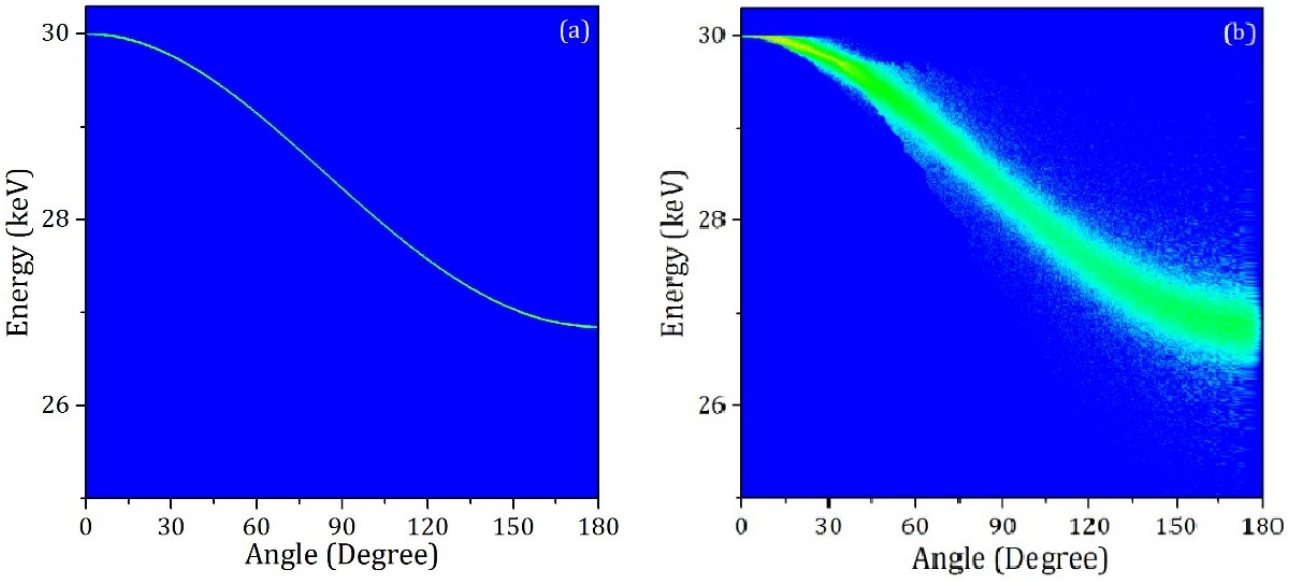

Figure 7: Double-differential distribution of the outgoing flux of gamma-rays as a function energy and angle, for incident photons with $E = 30$ keV.

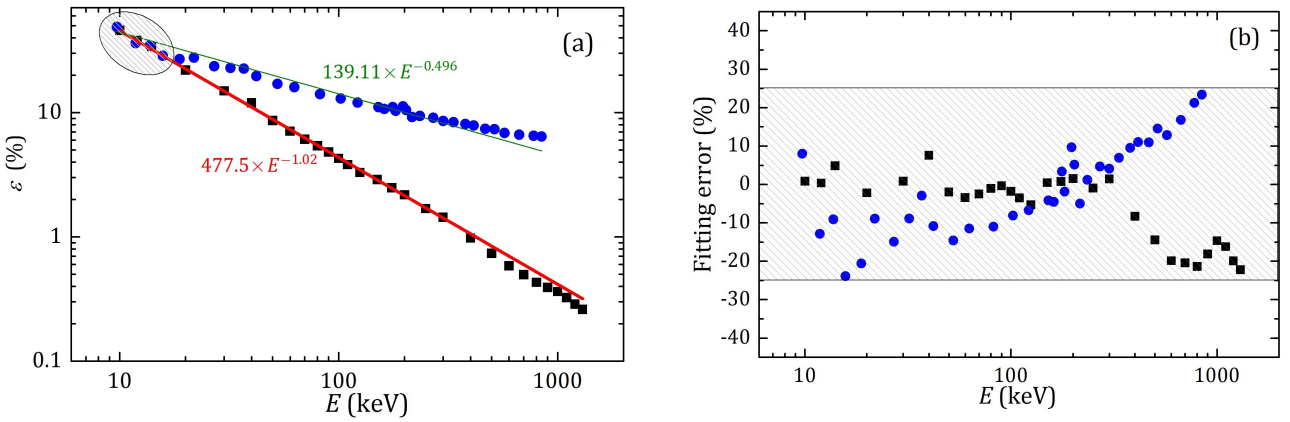

Figure 8: a) Energy resolution due to the Doppler broadening (■) as estimated in current study, and intrinsic energy resolution (●) as reported in (Swiderski et al., 2012). Continuous lines represent fitted curves. b) Corresponding error in the fitted curves.

ergy resolution, which is related to the population of received optical photons. Moreover, both data tend to similar values at lower energies (∼10 keV) that permit one to conclude about the significant role of the Doppler effect in such situations. It could be observed that the $1/E$ nature is more profound below 20 keV, emphasized by shaded region in Fig. 8-a. It is found that low-energy portion experimental data could be appropriately fitted by Eq. (16) with these parameters: $\alpha = 418.82 \pm 0.01$ and $\beta = -0.96 \pm 0.02$, persisting viability of $1/E$ nature for resolution in low-energy region.

5 Conclusions

A simple and accurate method based on the differentiation of the response function was proposed and detailed, aiming to localize and characterize the Compton edge. The method was also able to formalize the energy resolution of the detector as well. It has been examined by analyzing experimental measured data obtained by a BC400 plastic scintillation detector irradiated by different gamma-ray sources. Furthermore, based on extensive Monte Carlo simulations, we have determined Doppler energy resolution of the detector, which is shown to be principally originated from the boundedness of atomic electrons, tending to form. This conclusion is confirmed by comparison to the experimental data.

References

Beghian, L., Wilensky, S., and Burrus, W. (1965). A fast neutron spectrometer capable of nanosecond time gating. *Nuclear Instruments and Methods*, 35(1):34–44.

Bertin, A., Vitale, A., and Placci, A. (1969). A system of large liquid scintillation counters used with a simplified neutron-gamma discrimination technique. *Nuclear Instruments and Methods*, 68(1):24–38.

Böhlen, T. T., Ferrari, A., Patera, V., and Sala, P. (2012). Describing Compton scattering and two-quanta positron annihilation based on compton profiles: two models suited for the Monte Carlo method. *Journal of Instrumentation*, 7(07):P07018.

Briesmeister, J. F. (2000). MCNP Monte Carlo N-Particle Transport Code. *Version 4C, Los Alamos National Laboratory.*

Brown, J. M. C., Dimmock, M. R., Gillam, J. E., et al. (2014). A low energy bound atomic electron compton scattering model for Geant4. *Nuclear Instruments and Methods in Physics Research Section B: Beam Interactions with Materials and Atoms*, 338:77–88.

Brusa, D., Stutz, G., Riveros, J., et al. (1996). Fast sampling algorithm for the simulation of photon Compton scattering. *Nuclear Instruments and Methods in Physics Research Section A: Accelerators, Spectrometers, Detectors and Associated Equipment*, 379(1):167–175.

Chikkur, G. and Umakantha, N. (1973). A new method of determining the Compton edge in liquid scintillators. *Nuclear Instruments and Methods*, 107(1):201–202.

Cooper, M. J. (1997). Compton scattering and the study of electron momentum density distributions. *Radiation Physics and Chemistry*, 50(1):63–76.

Dietze, G. (1979). Energy calibration of NE-213 scintillation counters by δ-rays. *IEEE Transactions on Nuclear Science*, 26(1):398–402.

Dietze, G. and Klein, H. (1982). Gamma-calibration of NE-213 scintillation counters. *Nuclear Instruments and Methods in Physics Research*, 193(3):549–556.

Honecker, R. and Grässler, H. (1967). Detection efficiency of a plastic scintillator for neutrons between 0.2 and 3 MeV. *Nuclear Instruments and Methods*, 46(2):282–288.

Jolivette, P. and Rouze, N. (1994). Compton scattering, the electron mass, and relativity: A laboratory experiment. *American Journal of Physics*, 62(3):266–271.

Kippen, R. M. (2004). The GEANT low energy Compton scattering (GLECS) package for use in simulating advanced Compton telescopes. *New Astronomy Reviews*, 48(1-4):221–225.

Kling, A., Barao, F. J., Nakagawa, M., et al. (2014). *Advanced Monte Carlo for Radiation Physics, Particle Transport Simulation and Applications: Proceedings of the Monte Carlo 2000 Conference, Lisbon, 23–26 October 2000.* Springer Science & Business Media.

Knoll, G. F. (2010). *Radiation detection and measurement.* John Wiley & Sons.

Knox, H. and Miller, T. (1972). A technique for determining bias settings for organic scintillators. *Nuclear Instruments and Methods*, 101(3):519–525.

Kohan, M. R., Etaati, G., Ghal-Eh, N., et al. (2012). Modelling plastic scintillator response to gamma rays using light transport incorporated FLUKA code. *Applied Radiation and Isotopes*, 70(5):864–867.

Kornilov, N., Fabry, I., Oberstedt, S., et al. (2009). Total characterization of neutron detectors with a ^{252}Cf source and a new light output determination. *Nuclear Instruments and Methods in Physics Research Section A: Accelerators, Spectrometers, Detectors and Associated Equipment*, 599(2-3):226–233.

Namito, Y., Ban, S., and Hirayama, H. (1993). Implementation of linearly-polarized photon scattering into the EGS4 code. *Nuclear Instruments and Methods in Physics Research Section A: Accelerators, Spectrometers, Detectors and Associated Equipment*, 332(1-2):277–283.

Namito, Y., Ban, S., and Hirayama, H. (1994). Implementation of the Doppler broadening of a Compton-scattered photon into the EGS4 code. *Nuclear Instruments and Methods in Physics Research Section A: Accelerators, Spectrometers, Detectors and Associated Equipment*, 349(2-3):489–494.

Namito, Y., Hirayama, H., and Ban, S. (1998). Improvements of low-energy photon transport in EGS4. *Radiation Physics and Chemistry*, 53(3):283–294.

Pelowitz, D. B. et al. (2005). MCNPX users manual. *Los Alamos National Laboratory, Los Alamos.*

Roemer, K., Pausch, G., Herbach, C.-M., et al. (2010). Energy resolution and nonlinearity of NaI (Tl), CaF_2 (Eu), and plastic scintillators measured with the wide-angle Compton-coincidence technique. In *IEEE Nuclear Science Symposuim & Medical Imaging Conference*, pages 580–586. IEEE.

Safari, M., Davani, F. A., Afarideh, H., et al. (2016). Discrete fourier transform method for discrimination of digital scintillation pulses in mixed neutron-gamma fields. *IEEE Transactions on Nuclear Science*, 63(1):325–332.

Salvat, F. and Fernández-Varea, J. M. (2009). Overview of physical interaction models for photon and electron transport used in Monte Carlo codes. *Metrologia*, 46(2):S112.

Salvat, F., Fernández-Varea, J. M., and Sempau, J. (2006). PENELOPE-2014: A code system for Monte Carlo simulation of electron and photon transport. In *Workshop Proceedings*, volume 4, page 7.

Scintillators (2016). Plastic scintillators. http://www.crystals.saint-gobain.com/Plastic_Scintillators.aspx.

Sempau, J., Acosta, E., Baro, J., et al. (1997). An algorithm for Monte Carlo simulation of coupled electron-photon transport. *Nuclear Instruments and Methods in Physics Research Section B: Beam Interactions with Materials and Atoms*, 132(3):377–390.

Shenoi, B. A. (2005). *Introduction to digital signal processing and filter design*. John Wiley & Sons.

Sood, A. (2004). Doppler energy broadening for incoherent scattering in MCNP5, part I. *Los Alamos National Laboratory internal memorandum LA-UR-04-0488, Los Alamos, NM*.

Sood, A. (2009). Testing of Photon Doppler Broadening in MCNP5. 1.50 and MCNP5. 1.51. *Los Alamos National Laboraory*.

Sood, A. and White, M. C. (2004). Doppler energy broadening for incoherent scattering in MCNP5, part II. *Los Alamos National Laboratory internal memorandum LA-UR-04-0488, Los Alamos, NM*.

Stevanato, L., Fabris, D., Hao, X., et al. (2011). Light output of EJ228 scintillation neutron detectors. *Applied Radiation and Isotopes*, 69(2):369–372.

Swiderski, L., Marcinkowski, R., Moszynski, M., et al. (2012). Electron response of some low-Z scintillators in wide energy range. *Journal of Instrumentation*, 7(06):P06011.

Swiderski, L., Moszyński, M., Czarnacki, W., et al. (2010). Measurement of compton edge position in low-Z scintillators. *Radiation Measurements*, 45(3-6):605–607.

White, M. C. (2002). Photoatomic data library MCPLIB03: An update to MCPLIB02 containing Compton profiles for Doppler broadening of incoherent scattering. *Los Alamos National Laboratory internal memorandum X-5: MCW-02-110 (LA-UR-03-0787)*.

White, M. C. (2003). Photoatomic data library MCPLIB04: a new photoatomic library based on data from ENDF/B-VI release 8. *Los Alamos National Laboratory Memorandum No. LAUR-03-1019*.

White, M. C. (2012). Further notes on MCPLIB03/04 and new MCPLIB63/84 Compton broadening data for all versions of MCNP5. *Los Alamos National Laboratory technical report LA-UR-12-00018*.

Williams, B. (1977). Compton scattering: the investigation of electron momentum distributions.